Submarine spreading: Dynamics and development.

Aaron Micallef *, Douglas G. Masson, Christian Berndt and Dorrik A.V. Stow

National Oceanography Centre, European Way, Southampton, SO14 3ZH, UK.

Telephone: +44 23 80 596563; *Contact E-mail:amicall@noc.soton.ac.uk

Abstract

Spreading is a pervasive type of ground failure in subaerial environments, but its occurrence has hardly been documented in submarine settings. However, recent advances in seafloor imaging techniques show that repetitive extensional patterns of parallel ridges and troughs, oriented perpendicular to the direction of mass movement and typical of spreading, are widespread offshore. A spread develops via the failure of a surficial sediment unit into coherent blocks. These blocks are displaced downslope along a quasi-planar slip surface. Two modes of failure can be identified: retrogressive failure of the headwall, and slab failure and extension. Mechanical modelling indicates that loss of support and seismic loading are the main triggering mechanisms. The extent of displacement of the spreading sediment is controlled by gravitationally-induced stress, angle of internal friction of sediment, pore pressure escape and friction. The resulting block movement patterns entail an exponential increase of displacement and thinning of the failing sediment with distance downslope. A deeper insight into submarine spreading is important because of the widespread occurrence of ridge and trough morphology in numerous submarine slides, particularly in the vicinity of submarine infrastructures.

1. Introduction

Spreading involves the fracturing of a thin surficial layer of rock or soil into coherent blocks and their finite lateral displacement on gently sloping ground (Varnes 1978). The associated ground deformation is generally characterised by extensional fissures, resulting in a series of parallel ridges and troughs at the surface (Bartlett and Youd 1995). Recent advances in acoustic data acquisition techniques allow the identification of ridge and trough morphology within the Storegga Slide. Located on the mid-Norwegian margin, the Storegga Slide occurred 8100±250 cal. yrs BP as sixty-three quasi-simultaneous slide events (Haflidason *et al.* 2005). It is one of the largest known submarine mass movements, and it has been thoroughly surveyed by state-of-the-art acoustic imagery. Spreading has seldom been observed in the submarine realm, and the Storegga Slide provides an ideal setting for a deeper investigation of this type of mass movement. The objectives of this study are to identify the mechanisms that give rise to submarine spreading, and to characterise the associated morphology.

2. Data sets

There are three acoustic data sets available for this study (Figure 1a). The first consists of high resolution multibeam bathymetry that covers the Storegga Slide scar with a horizontal resolution of 25 m or better. The second comprises Towed Ocean Bottom Instrument (TOBI) sidescan imagery of 60% of the slide scar. The nominal resolution of these data is 6 m. The third data set consists of high resolution 2D seismic lines located in the northeast of the slide scar.

Fig. 1

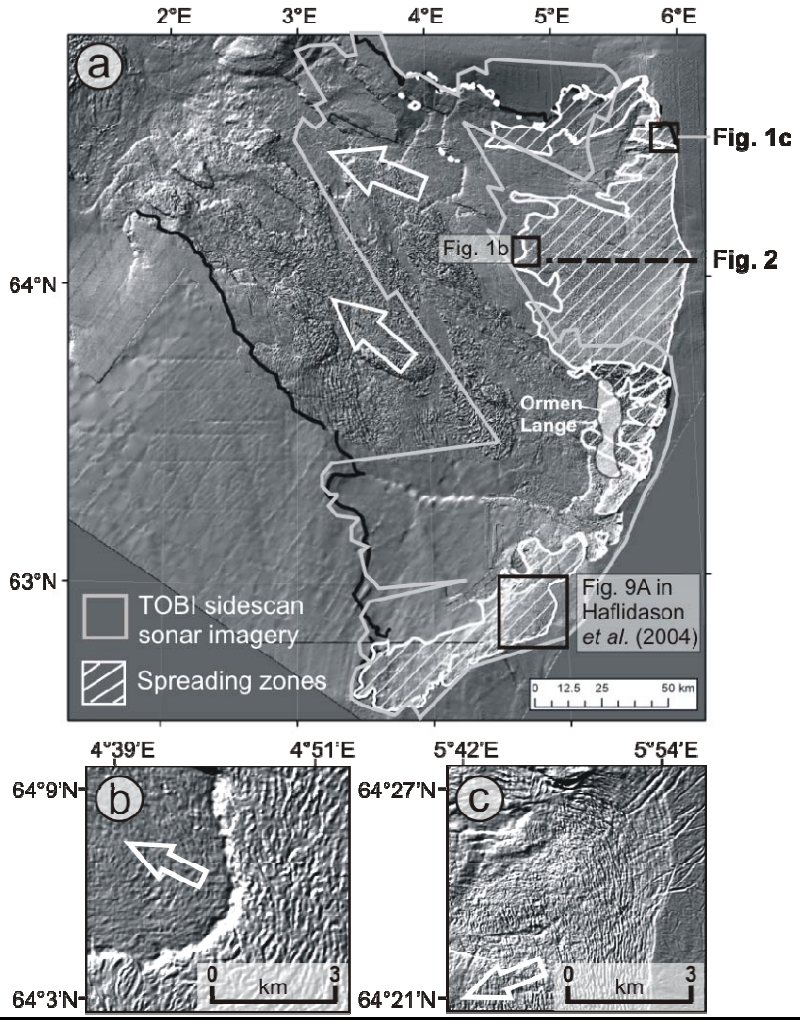

Figure 1: (a) Shaded relief map of the Storegga Slide (illumination from NW, 3× exaggeration), showing the zones of spreading and the coverage of TOBI sidescan sonar imagery. (b) Enlarged section of the shaded relief map from the distal part of a spread, where a steep and high escarpment is located. Upslope of the escarpment, the ridges are clearly visible and closely spaced, whereas downslope of the escarpment the morphology is more subdued and blocky. (c) Enlarged section of the shaded relief map from the upper part of a spread, close to the main headwall. The ridge pattern, which is more closely spaced in this region, is intersected by a number of iceberg ploughmarks. These are older than the spread and demonstrate the limited extension that has taken place near the headwall. The white arrows indicate the direction of sediment mobilisation. Also shown is the location of Figure 9a in Haflidason *et al.* (2004), which is a good example of sidescan sonar imagery of the ridge and trough morphology from the southern part of the Storegga Slide.

3. Results

Ridge and trough morphology is widespread within the Storegga Slide (Figure 1). The ridges and troughs are generally aligned parallel to a headwall. The plan pattern of the ridges and troughs is concave-downslope in the upper parts of the slope, changing to linear or convex-downslope with increasing distance from the headwall.

A vertical profile of the ridge and trough morphology in one of the high resolution seismic lines is shown in Figure 2. The seismic section consists of an upper sequence of downslope dipping reflectors, located at the top of reflector packets dipping at a similar downslope

gradient. The reflector packets are separated by a series of upslope dipping reflectors (Figures 2b and 2d). At the bottom of the seismic section are four quasi-planar continuous reflectors. The upper seismic reflectors and the reflector packets are slightly steeper dipping than the bottom reflectors (Figures 2b and 2d). The reflectors in this seismic section are interpreted as layers in a stratified sediment package. This package is undeformed in the deeper parts, whereas it is broken up into blocks in the shallower parts. The lengths of these blocks were estimated at ~130 m. Using an acoustic velocity of 1700 ms^{-1} for the sediments, the mean slope gradient of the surface of the undeformed section was estimated at 1°. The estimated thickness of the failing sediment decreases gradually from 80 m in the upslope part of the seismic line, to 25 m in the downslope part (Figure 2c). The dips of the interfaces between the blocks have an average angle of ~25°. We interpret the blocks as having translated along a quasi-planar slip surface as the sediment unit was extended. During this displacement, the blocks have tilted anticlockwise and downslope, and in the process the upper part of the blocks has been exposed. This has resulted in a step-like morphology that is responsible for the ridges and troughs at the surface. The block pattern is best preserved close to the headwall, and there is progressive deformation of the blocks with distance downslope (Figure 2a).

Having established that the ridge and trough morphology is representative of spreading, we mapped the spatial extent of this mass movement across the Storegga Slide (Figure 1a). Ridge and trough morphology can be observed over a total area of 6000 km^2, or ~25% of the slide scar. It is mainly located along the main Storegga headwall, in the northeastern and southern parts of the slide scar. The spreading regions are generally bounded by a gentle, shallow headwall at their upslope limit (Figure 1c), and a steep, high escarpment at their downslope limit (Figure 1b). In the upslope sections, a number of iceberg ploughmarks, older than the Storegga Slide, can be identified, which are indicative of the limited displacement of the sediment (Figure 1c). Downslope of the distal escarpment, the surface is characterised by either blocks or very subtle ridges (Figure 1b).

Ridge and trough morphology varies across the spread in Figure 2a. The depth of the troughs shows a general increase from 1.5 m near the headwall to 5.5 m towards the toe. The length of individual ridges along the crest decreases from 360 m upslope to 250 m downslope. The number of ridges per unit area increases away from the headwall, reaching values of up to 12 km^{-2}. Spread morphology also varies across the Storegga Slide, with ridges in the Ormen Lange region being longer, more widely spaced, and having troughs up to 3× deeper than elsewhere. In the Ormen Lange region, the downslope face of the ridges is steeper than the upslope face. Failure takes place in the deep and thick O4-O7 sediments (200-130 ka) of the Naust formation, which consist of glacial till and debris flow deposits (Berg *et al.* 2005). The ridges in the rest of the spreading zones are shorter, more closely spaced and have shallower troughs. The downslope face of these ridges is gentler than the upslope face, and failure takes place in the shallow and thin O1-O2 sediments (30-15 ka), consisting of basal and deformation till, and O3 sediments (130-30 ka), which are fine-grained hemipelagic and glacial marine clays (Bryn *et al.* 2005) (for more information on the Storegga Slide stratigraphy refer to Berg *et al*. (2005)).

Fig. 2

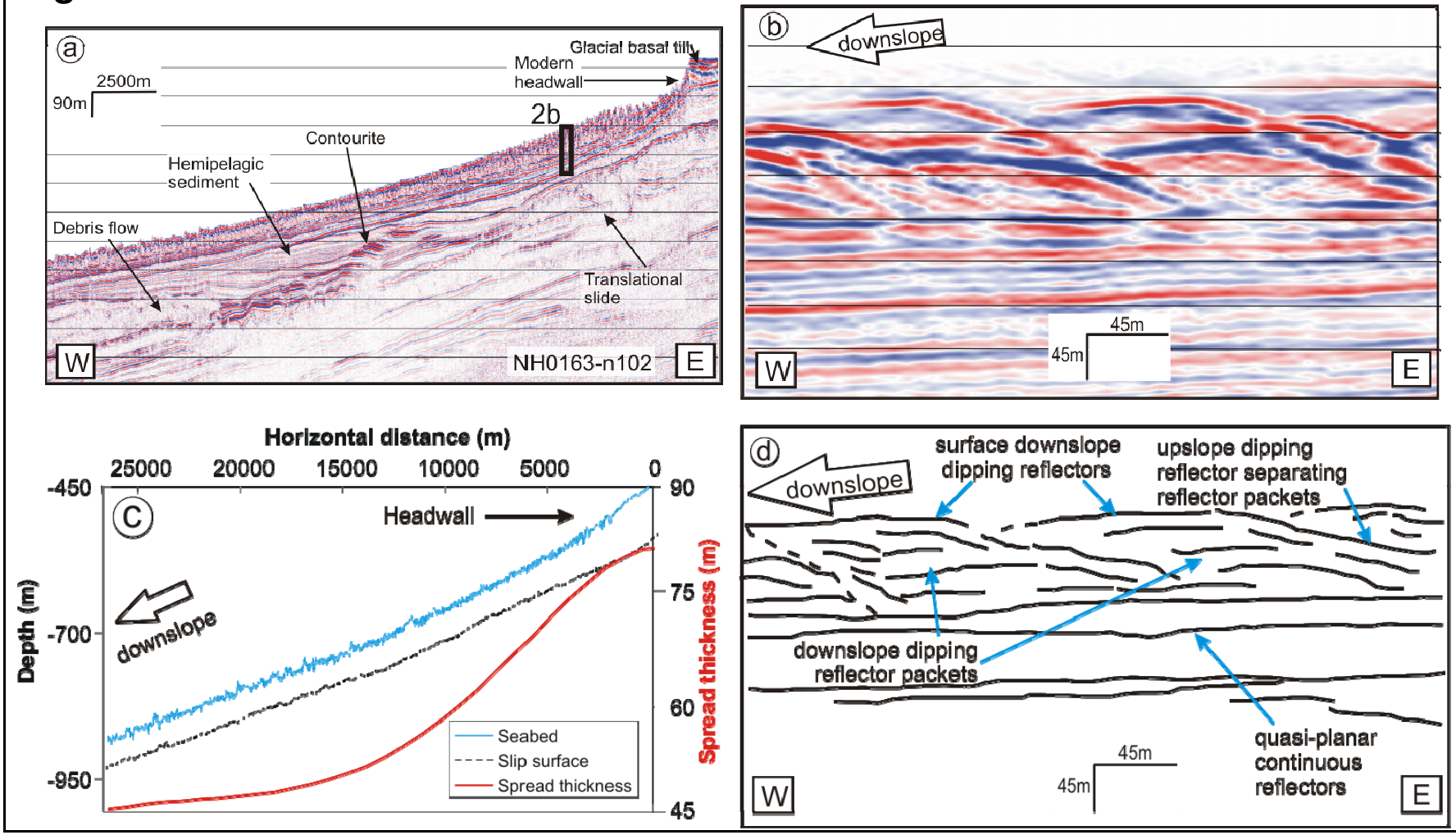

Figure 2: (a) Annotated profile of seismic line NH0163-n102; location is shown in Figure 1a. (b) Enlarged section of a part of the seismic profile, showing the internal structure of the ridge and trough morphology. (c) Interpreted seabed and slip surface of the seismic profile in Figure (a), and the calculated thickness of the spreading sediment. (d) Labelled interpretation of the enlarged seismic section in (b). See section 3 for a more detailed explanation.

4. Discussion

4.1 Mode of failure

We propose two models for the failure dynamics of spreading based on the morphology and internal structure of the ridges within the Storegga Slide (Figure 3). The first model (model 1) entails failure in a thin slab of sediment underlain by a failure plane or 'weak layer'. The slab, which is under tension, breaks up into a series of coherent blocks, with shear planes dipping upslope (Figure 3a). This occurs because of extensional forces that are higher downslope and basal resisting forces that are stronger upslope (due to, for example, changes in the thickness of the failing layer (Berg *et al.* 2005) and/or a decrease in excess pore pressure with distance upslope (Strout and Tjelta 2005)). Failure can initiate anywhere along the slope. In the Ormen Lange region, the ridge morphology is different. Failure in this region can be explained by the model of Kvalstad *et al.* (2005) (model 2) where spreading propagates upslope via the repeated unloading of the headwall and the fracturing of the sediment into blocks (Figure 3b). The shear planes dip downslope and the blocks are rotated in a clockwise direction. The difference in the mode of failure is explained by the different properties of the failing sediment, with the failing sediment in the Ormen Lange being thicker and having lower clay content (Berg *et al.* 2005).

Fig. 3

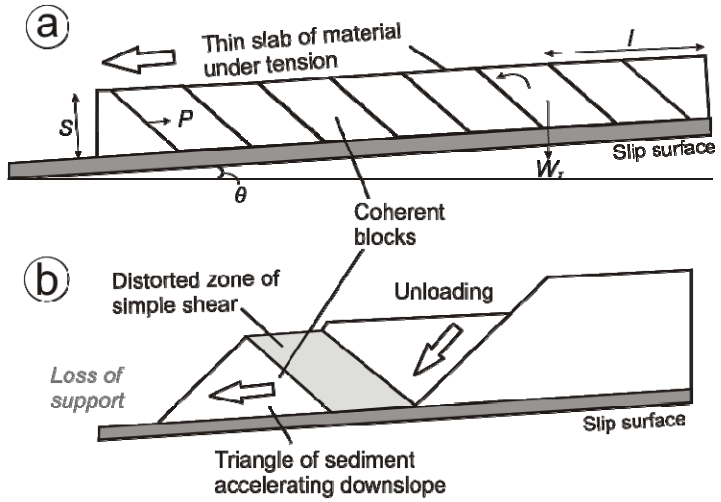

Figure 3: Schematic illustration of the two models of failure: (a) model 1 (slab extension and rupturing); (b) model 2 (repeated failure of the headwall). Figure (a) also shows some of the static forces and dimensional attributes considered in the limit-equilibrium model. Figure (b) is adapted from Kvalstad *et al.* (2005).

4.2 Triggers of a spread

Both models of failure can be modelled using a limit-equilibrium model (Figure 3a). We considered the driving and resisting forces acting on a series of equidimensional blocks resting on a planar slip surface:

Driving forces:

$$Sin\theta\ (W_T) \qquad (1)$$

Resisting forces:

$$Tan\ \phi\ [W_T(Cos\ \theta) - u] + c + P \quad (2)$$

W_T total weight of sediment upslope of a block = γSl
γ submerged unit weight (in 2D)
S sediment unit thickness prior to failure
l distance from a fixed point upslope
θ slope gradient of slip surface
ϕ angle of internal friction
u pore water pressure (in 2D)
c cohesion
P supporting force from slab downslope

The factor of safety of this model will decrease if there is: (a) a decrease in P; (b) an increase in u; (c) an increase in W_T; (d) an increase in γ; (e) an increase in S; (f) an increase in l; (g) an increase in θ; (h) a decrease in ϕ; and/or (i) a decrease in c. A slope failure can be initiated by a temporal change in one/many of these variables, if the magnitude of the change is such that the factor of safety decreases below zero. Therefore, a spread within the Storegga Slide can be triggered by:

(a) Loss of support at the base of the slope, caused by a slope failure occurring downslope of the sediment unit affected by spreading. This is likely to be an important trigger within the Storegga Slide because a steep escarpment is located in the distal edge of most spreading zones.
(b) Increase in the total weight of sediment upslope, due to loading of sediment from a slope failure located upslope of the spreading sediment unit. There are no indications that this is a significant trigger within the Storegga Slide.
(c) Seismic loading, caused by the glacio-isostatic rebound following the deglaciation of Scandinavia (Atakan and Ojeda 2005), may have induced downslope shear stresses, leading to short term failure and strength loss, and/or increase in pore pressure.

4.3 Pattern of block displacement

We apply equations of motion to the blocks in Figure 3a to infer their behaviour during spreading. We can calculate the acceleration, velocity and distance travelled by individual blocks if we assume that the failure was instantaneous, and that fluid resistance and friction at the base are constant along the entire slip surface. We estimate the values for the different variables in the model from a 35 km section of the seismic line NH0163-n102. The blocks are 130 m wide, and θ and S are constant at 1º and 80 m, respectively. γ and ϕ increase upslope from 9 kN m^{-2} to 10 kN m^{-2}, and from 25º to 27.5º, respectively. The reason for this variation is that the sediments become more consolidated upslope towards the shelf edge due to compaction by glacial advance during glacial maxima. u increases from 1000 kN m^{-2} downslope to 600 kN m^{-2} upslope, due to unloading of the sediment in the upslope region after the Last Glacial Maximum (Strout and Tjelta 2005). c is constant at 7 kPa (Sultan *et al.* 2004).

Changes in the velocity and distance covered by individual blocks along a section of the slope, after a spread is triggered, are shown in Figure 4a. The first block to be released (block 1) attains the highest velocity and covers the longest distance. This is because in the

downslope section of the slope, W_T, l and u have high values, and γ and ϕ have low values, creating the conditions for the highest resultant force. The values of W_T, l, u, γ and ϕ change with distance upslope, resulting in a lower velocity attained and lower distance covered by successive blocks. The variation of block displacement with distance downslope is an exponential increase (Figure 4b).

Fig. 4

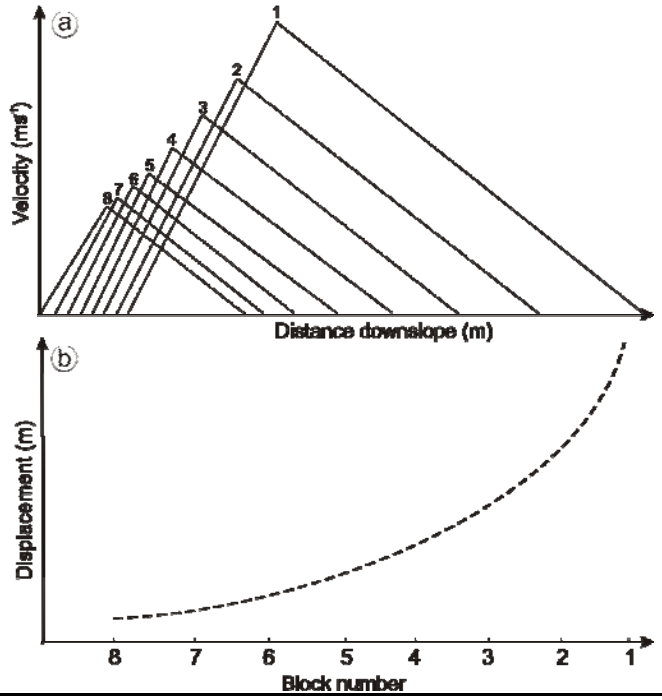

Figure 4: (a) Plot of velocity vs. distance downslope for a number of blocks in a theoretical spread, using values from the Storegga Slide. Block number indicates the order in which the blocks are displaced. (b) Exponential variation of block displacement with block number.

According to this model, the velocity of the blocks and the distance they cover should increase continuously with distance. This is not the case because the distal remnants of spreads can be identified downslope of the distal escarpment. As the spreading sediment collapses over the escarpment, the blocks fragment. This allows the escape of excess pore pressure from the base of the spread, which reduces the velocity of the blocks. The sediment remaining upslope of the distal escarpment is likely to be slowed down by loss of excess pore pressure via the remoulding of sediment due to friction. Furthermore, as the spreading unit extends and breaks up, it also becomes thinner (Figure 2c). The decrease in S reduces the gravitationally-induced stress and retards block displacement further.

5. Conclusions

Spreads within the Storegga Slide are most probably triggered by either a loss of support due to mass movements taking place downslope of a spreading unit, or by seismic loading. When a spread is triggered, shear planes and coherent blocks form within the sediment unit. The mode of failure involves either the retrogressive failure of the headwall, as for the Ormen Lange region, or slab extension and rupturing, as for the rest of the spreading zones. The blocks in the distal edge of the spread are displaced the most and generally collapse over a pre-existing escarpment. The sediment either preserves the ridge and trough

morphology or develops into a debris flow. In the remaining part of the spread located upslope of the distal escarpment, extension, friction and water resistance combine to fragment and remould the sediment blocks as they are displaced downslope. Loss of excess pore pressure and thinning of the sediment unit retard the blocks and finally bring them to a halt. Block disintegration, displacement and velocity decrease exponentially upslope until a gentle headwall is formed. Within Storegga, this pattern is controlled by changes in pore pressure, gravitationally-induced stress, and the angle of internal friction of the sediment.

A recurrent extensional pattern of parallel ridges and troughs, oriented perpendicular to the direction of movement, can be observed in numerous well-known submarine slides around the world (e.g. Trænadjupet Slide in Laberg *et al.* (2002); Nyk Slide in Lindberg *et al.* (2004); BIG'95 Slide in Lastras *et al.* (2003); Hinlopen Slide in Vanneste *et al.* (2006)). This may indicate that spreading is a widespread type of submarine mass movement. Spreading tends to occur on gentle terrain over extensive regions, some of which are located in the vicinity of oil and gas exploitation infrastructure (e.g. Ormen Lange). A better understanding of spreading as a potential geohazard, and its role in the evolution of submarine slides, is thus pertinent.

6. Acknowledgements

We are grateful to Norsk Hydro AS for providing the bathymetric data and the high-resolution 2D seismic lines. European North Atlantic Margin (ENAM) II Programme is acknowledged for making the TOBI sidescan sonar imagery available.

7. References

Atakan, K. and Ojeda, A., 2005. Stress transfer in the Storegga area, offshore mid-Norway. *Marine and Petroleum Geology*, 22(1-2): 161-170.

Bartlett, S. F. and Youd, T. L., 1995. Empirical prediction of liquefaction-induced lateral spread. *Journal of Geotechnical Engineering*, 121(4): 316-329.

Berg, K., Solheim, A. and Bryn, P., 2005. The Pleistocene to recent geological development of the Ormen Lange area. *Marine and Petroleum Geology*, 22(1-2): 45-56.

Bryn, P., Berg, K., Forberg, C. F., Solheim, A. and Kvalstad, T. J., 2005. Explaining the Storegga Slide. *Marine and Petroleum Geology*, 22(1-2): 11-19.

Haflidason, H., Lien, R., Sejrup, H. P., Forsberg, C. F. and Bryn, P., 2005. The dating and morphometry of the Storegga Slide. *Marine and Petroleum Geology*, 22(1-2): 123-136.

Haflidason, H., Sejrup, H. P., Nygård, A., Bryn, P., Lien, R., Forsberg, C. F., Berg, K. and Masson, D. G., 2004. The Storegga Slide: Architecture, geometry and slide-development. *Marine Geology*, 231: 201-234.

Kvalstad, T. J., Andersen, L., Forsberg, C. F., Berg, K., Bryn, P. and Wangen, M., 2005. The Storegga slide: evaluation of triggering sources and slide mechanisms. *Marine and Petroleum Geology*, 22(1-2): 245-256.

Laberg, J. S., Vorren, T. O., Mienert, J., Evans, D., Lindberg, B., Ottesen, D., Kenyon, N. H. and Henriksen, S., 2002. Late Quaternary palaeoenvironment and chronology in the Trænadjupet Slide area offshore Norway. *Marine Geology*, 188: 35-60.

Lastras, G., Canals, M. and Urgeles, R., 2003. Lessons from sea-floor and subsea-floor imagery of the BIG'95 debris flow scar and deposit. *In:* Locat J, Mienert J (eds) *Submarine Mass Movements and Their Consequences*. Kluwer Academic Publishers, Dordrecht, pp 425-431.

Lindberg, B., Laberg, J. S. and Vorren, T. O., 2004. The Nyk Slide - morphology, progression, and age of a partly buried submarine slide offshore northern Norway. *Marine Geology*, 213: 277-289.

Strout, J. M. and Tjelta, T. I., 2005. In situ pore pressures: What is their significance and how can they be reliably measured? *Marine and Petroleum Geology*, 22(1-2): 275-285.

Sultan, N., Cochonat, P., Foucher, J. P. and Mienert, J., 2004. Effect of gas hydrates melting on seafloor slope instability. *Marine Geology*, 213: 379-401.

Vanneste, M., Mienert, J. and Bünz, S., 2006. The Hinlopen Slide: A giant, submarine slope failure on the northern Svalbard margin, Arctic Ocean. *Earth and Planetary Science Letters*, 245(1-2): 373-388.

Varnes, D. J., 1978. Slope movement types and processes. *In:* Schuster RL, Krisek RJ eds) *Landslides, Analysis and Control*. National Academy of Sciences, Transportation Research Board, Special Report 176, pp 11-33.